CHAPTER V

ENHANCEMENT OF ANTI - CORROSION PROPERTIES OF EPOXY SYSTEM WITH DISPERSED *Senna auriculata* INCORPORATED NANOCLAY FOR MILD STEEL IN ALKALINE AND ACID ENVIRONMENTS

5.1 Introduction

Mild steel is an utmost metal used in the fabrication of materials, automobiles, petroleum refineries etc., but it is easily vulnerable to corrosion. Metal corrosion in industrial zone is a serious worldwide issue leading to monetary loss of a country's economy. To mitigate corrosion, organic coatings can be applied on the metal which tends to form a physical barrier between the metal and corrosive environment[1,2]. The efficacy of coatings has been influenced by some factors such as nature and suitability of the material, methodology used for incorporating the inhibitor and environmental factors[3,4]. A good coating should possess the following requirements such as long lasting, eco-friendly, low cost, easy to apply and high performance. In this context, epoxy resins play a vital role in protecting the metal from corrosion due to its superior mechanical, dielectric, heat and anti-corrosive properties[5]. In general, epoxy coatings decrease the corrosion rate as they act as a physical barrier to impede the entry of detrimental species[6,7]. The performance of the epoxy coatings depends on their vulnerability to water uptake, wear resistances and surface abrasion. Consequently, certain materials are added to epoxy coating to enhance their corrosion resistance and physical properties. Inspite of these efficient properties of epoxy coatings, they fail due to the inadequate barrier performance of the film resistant to corrosive species. Due to the dissemination of the corrosive agents into the epoxy/metal interface blistering occurs and interfacial adhesion bond devastation takes place at prolonged exposure times. In order to enrich the corrosion resistance performance of the coating several methods are available. The most commonly used method to induce corrosion protection performance in the epoxy coating is the incorporation of nanoparticles, capsules and pigments[8,9]. Pigments based on chromates enhance an active corrosion protection in epoxy coatings but due to their high deleterious effects their usage is limited and researchers are instigated on promoting eco-friendly corrosion retarding systems[10,11]. A promising

approach is to use nanoclay which is a pervasive nanofiller that belongs to the category of clay minerals thus natural, ample, eco-friendly, less expensive material and finds application in many fields such as medicine, cosmetics, catalysis, textile, industries etc.,. The special nature of the montmorillonite nanoclay is greater surface area, small particle size and ion-exchange properties. It also possess dioctahedral geometry by 2:1 layer linkage. Furthermore, to increase the dispersability and inhibition properties of the clay in the epoxy resin, some modifications should be carried out on the surface of the clay. Usage of inhibitors is one of the prominent method in modifying the MMT clay[12,13]. In most cases the active inhibitor compounds are held by the clay polymer chain and are not able to disperse through the organic coating to arrive at the metal/layer interface to impede the corrosion reactions. To overcome this problem, the inhibitor molecules are blended into the clay backbone and the modified clay is dispersed in the organic coating. Inhibitors extricate slowly at the metal/film interface and react with substrate to afford protection against corrosion[14]. Natural and synthetic inhibitors can be used to modify the clay. Synthetic inhibitors possess excellent corrosion inhibition effects but they are highly baleful, expensive, time consuming, posing threats to human life and environment during their implementation. Hence in this study eco-friendly, plenteous, cheap *Senna auriculata* leaves were used. It belongs to the family fabaceae. It grows up to a height of 31 to 60 cm. Leaves are yellowish green in colour. It grows easily on black soil and is also found near railway embankments. It has tremendous medicinal values such as treating diabetes, fungal infection, liver toxicity etc.,[15]. Limited number of research works have focussed on epoxy resin with modified clay and previous literature review is presented below.

5.2 Review of literature

Raju *et al.*, investigated a series of nanoclay polystyrene nanocomposite coatings for anticorrosion applications. The corrosion properties were investigated by electrochemical methods such as electrochemical impedance spectroscopy and potentiodynamic polarization studies in 3.5 wt% of NaCl medium. A significant enhancement in properties like corrosion protection, thermal stability, optical density was evaluated[16].

Hosseini *et al.*, evaluated the anti-corrosion performance of epoxy/polyaniline-imidazole modified ZnO nanocomposite on mild steel in NaCl by electrochemical

impedance spectroscopy. Nanocomposites were prepared by in-situ emulsion polymerization method and it was characterized by IR and SEM analysis. The results exhibited better corrosion resistance with higher barrier properties against aggressive ions[17].

Vijayakumar *et al.,* determined the compression strength of composites (epoxy nanoclay) in salt laden atmosphere. The compressive strength was evaluated before and after the epoxy nanoclay composites were subjected to salt spray test[18].

Wan *et al.,* incorporated paint with henna extract. The extract was characterized using FT-IR techniques. The inhibitory action of henna extract of concentration (0, 4, 8, 10%) was incorporated into epoxy based matrix and analysed by electrochemical technique. The surface morphology was studied by using SEM. It has been found that the protection efficiency was increased as concentration was increased[19].

Ghodrati *et al.,* modified montmorillonite (MMT) with hexadecyltrimethyl ammonium bromide (HDTB) and utilized as a nano-additive for improvement of anti-corrosion and mechanical properties of epoxy coating. The modified HDTB was analysed using IR, thermogravimetric analysis, XRD and TEM analysis. The results from electrochemical studies and salt spray tests indicated an increased corrosion resistance of modified clay/epoxy coating[20].

Relosi *et al.,* incorporated the nanofillers (muscovite mica and montmorillonite) and dispersed in epoxy coating to increase the properties of the coating. The coatings were characterized by mechanical, thermal and chemical analysis. The incorporation of clay into epoxy coating improved the roughness of the surface leading to a diffuse in reflection of incident light and on gloss reduction[21].

Madhup *et al.,* loaded diglycidyl ether bisphenol A based epoxy resin with alkyl quaternary ammonium modified bentonite clay nanoparticles (b-CNPs) at different concentrations. The property of composite coatings such as abrasion resistance were evaluated. It has been found that the abrasion resistance increases as concentration of CNP increased. The developed epoxy nanocomposite was characterized by thermal (DSC), FT-IR and SEM studies. SEM analysis indicated a smooth film morphology due to uniform distribution of b-CNPs inside polymer nanocomposite matrix[22].

Shankar *et al*., incorporated conventional alumina and montmorillonite nanoclay into aqueous epoxy emulsion by ultra-sonication process. The nanocoatings were deposited on copper metal cathode and parameters such as alumina content, pH, nanoclay content were studied. The results revealed that epoxy alumina-MMT nano coatings showed superior corrosion resistance than epoxy coating. The strength of the epoxy alumina - montmorillonite nanocoatings was improved compared to pure epoxy coating[23].

Jlassi *et al*., prepared epoxy polymer nanocomposites filled with magnetite (Fe_3O_4) clay at different filler loading of 0.1, 0.5, 1, 3, 5 wt%. The modification of clay by polyaniline was done by using 4-diphenylaminediazonium salt (DPA). Tensile strength, dielectric and mechanical properties was studied. The results from EIS studies insisted an enhancement in anti-corrosion property in NaCl medium was noticed. The charge transfer resistance is much higher for 3 wt% filler than pure epoxy[24].

Gul *et al*., synthesized nanobifiller (Bentonite clay modified organically with quaternary salt of threonine amino acid and nano diamolecules) filled epoxy, nylon 66 by casting method and evaluated corrosion resistance and abrasion resistance for aerospace and automotive applications. Different techniques like impedance spectroscopy and salt spray analysis were adopted to investigate the corrosion mitigation performance of prepared samples[25].

Mahmoodi *et al*., prepared epoxy/nanopigment coatings and evaluated their physical and mechanical properties. Nano pigments were synthesized by cationic exchange reaction between methylene blue and cloisite clay. Techniques adopted for the analysis included CHNS, TEM, XRD, DMTA, QUV accelerated weathering tester and spectrophotometry. The colour and mechanical properties of epoxy/nano pigment coatings were found to be superior than reference coatings[26].

3-Aminopropyltriethoxysilane was incorporated into Halloysite nanoclay by **Rudresh *et al*.,** and modified clay was analysed by powder XRD, SEM, FT-IR. The effect of modified clay on mechanical behavior of epoxy/nanoclay composites was studied at various concentrations such as 2%, 3%, 4% and 5% of HNPs in the epoxy resin. The results revealed that 4 wt % of HNPs showed maximum improvement in mechanical properties of epoxy[27].

Nguyen *et al*., prepared epoxy resin/epikote nanoclay/multiwalled carbon nanotube nanocomposite by mechanical stirring method and reported the enhancement of mechanical and flame retardant properties. It has been found that the prepared material exhibited higher thermal and mechanical properties and high potentiality hence it can be applied for multifaceted applications[28].

Akbarinezhad investigated the protective properties of an epoxy zinc-rich primer (ZRP) modified with polyaniline (pani) and exfoliated polyaniline graphite nanocomposites. The aggressive medium was 3.5% NaCl and corrosion resistance properties were evaluated by electrochemical noise and electrochemical impedance spectroscopy (EIS). The results revealed that the barrier properties of ZRP primer was enhanced after the addition of nanocomposites to ZRP primer[29].

Zhang *et al*., prepared polyurethane modified epoxy (WPUME) emulsion, a corrosion resistant waterborne. It was characterized by FT-IR, TEM and TGA analysis. By weighing method and laser-scattering equipment the particle size, dispersion as well as the solid content of the emulsion were determined. By standard methods water absorption rate, flexibility and salt spray resistance were analyzed. The results exposed that coated plates have good flexibility and able to withstand for longer times[30].

Kabeb *et al*., developed a nanocomposite coating with graphene nanoplateles (GNP) and montmorillonite (MMT) by mechanical agitation process to improve the corrosion resistance and flame retardancy of mild steel samples. The analysis such as salt fog test, water absorption and limiting oxygen index indicated that presence of little amount of filler resulted in remarkable enhanced anti-corrosion property and flame retardancy of epoxy nanocomposites[31].

Truc *et al*., inserted 8-hydroxyquinoline (8HQ) into montmorillonite platelets (8HQ-MMT) and clay was modified and incorporated into epoxy and deposited on carbon steel substrates. The anti-corrosion property of 8HQ-MMT was analysed by electrochemical methods in 0.1 M NaCl solution on bare carbon steel. The epoxy containing ammonium quaternary salt - modified clay was taken as reference sample and results were compared[32].

The present study focuses on enhanced corrosion protection by natural inhibitors, incorporated into the lattices of nanoclay which forms an ideal combination for high

corrosion protection of equipment and structures against severe corrosive environments. In this regard, a green inhibitor (*Senna auriculata*) was used to enhance the anti-corrosion properties of epoxy resin.

5.3 Materials and methods

5.3.1 Preparation of inhibitor

Senna auriculata (SA) leaves were washed thoroughly with distilled water to remove dust particles and dried at room temperature (303±1K). The dried leaves were pulverized into a powder form. About 1.5 g of powdered material was added to 150 ml of double distilled water, refluxed for 3 hours at 70^{o}C. After cooling, it was filtered and the filtrate was used as the inhibitive solution.

5.3.2 Preparation of SA- modified clay

Montmorillonite nanoclay (5-100 nm) was purchased from M/s Platonic nanotech. Nanoclay (1.5 g) was dispersed in 150 ml of inhibitor solution and 0.25 ml of concentrated hydrochloric acid was added. The solution was stirred at 80^{o}C for 24 hours which imparted a brown precipitate. The brown precipitate was filtered and washed with double distilled water. 0.1 M silver nitrate was added to the filtrate until no chloride was identified[33]. SA-modified clay was dried in hot air oven at 80^{o}C for 2 days. **Figs. 5.1a and 5.1b** represent clay and SA modified clay.

5.3.3 Preparation of electrolyte and working electrodes

The electrolytes used for the corrosion analysis were 0.5 M NaCl (alkaline) and 0.5 M H_2SO_4 (acid). The mild steel of composition (in weight %) are 0.085 C, 0.368 Mn, 0.128 Si, 0.024 P, 0.026 S, 0.023 Cr, 0.012 Mo, 0.014Ni and 98.9% Fe was used for corrosion analysis. Specimen of size 3 cm x 1 cm x 0.1 cm was utilised.

5.3.4 Preparation of coating solution

Epoxy resin (epoxy equivalent 450-500) was procured from M/s Resins & Plastics Ltd., Mumbai, and polyamide resin (Amine value 300) from M/s Ciba Atul Industries, Mumbai. Epoxy resin is the base and polyamide resin is the hardener (or) activator. About 1.5 g of SA-modified clay was dispersed in 35 g of epoxy resin taken in a beaker. The system was dispersed in a sonicator for 8 hours. The dispersion was continued until

the system became completely homogenous. A small quantity of solvent was added to maintain the consistency. Then 15 g hardener was added to this solution and mixed well. After maturation for about 20 minutes the system was applied on MS panels and cured for 7 days. The dried panels were used for various tests.

5.3.5 Spectral analysis

5.3.5.1 Gas chromatography - mass spectrometry analysis (GC-MS)

The biocompatible phyto constituents in *S. auriculata* extract were evaluated by using Perkin Elmer Clasus 60 GC-MS instrument. The specifications are 30 m, id 0.25 mm, 0.25 μm film and 1 microliter injection volume was utilised with carrier gas as helium at 1 ml/min. The analysis of the phyto constituents was carried out by applying 70 eV ionization energy. Analysis of the sample was done for 40 minutes. Phyto constituents in the extract were examined with NIST data references.

5.3.5.2 Infrared and UV-Visible spectroscopy analysis

FT-IR spectra of *S. auriculata* leaves extract was recorded to detect the presence of active species which contribute for the efficient working of the inhibitor. The spectra was recorded in the frequency range 4000 - 400 cm^{-1} using ATR-IR Affinity-1 (Schimadzu, Japan). UV spectra of the leaf extract was recorded using UV 3000 LAB INDIA.

5.3.6 Electrochemical techniques

5.3.6.1 Electrochemical impedance spectroscopy (EIS)

EIS technique is a powerful tool for identifying the corrosion process and also for analysing reaction mechanism[34]. A three electrode cell system with calomel electrode as reference, platinum electrode as counter and coated samples as working electrode was used. Electrochemical data was obtained at open circuit potential (OCP) by Metro ohm auto lab instrument with NOVA software in the frequency range of 10 kHz to 0.01 Hz with amplitude of 10 mV. The cell assembly was open to air and the analysis was done at room temperature (303±1K). The corrosive medium was 0.5 M NaCl and H_2SO_4 solutions. Samples (epoxy-clay coated system, SA-epoxy coated systems) coated on mild steel plates were dipped in 100 ml of 0.5 M NaCl and 100 ml of 0.5 M H_2SO_4 and EIS measurements were carried over time.

5.3.6.2 Potentiodynamic polarisation studies

Polarisation studies provide information on the ability of the coating to impede corrosion against a voltage gradient. The setup used for EIS measurements was used for recording polarisation curves. Corrosion kinetic parameters $I_{corr,}$ E_{corr} and Tafel slopes (b_a, b_c) can be determined for the coated samples both in the presence and absence of inhibitor. Tafel curves were assessed over the potential range of +200 mV to -200 mV with respect to the OCP at a scan rate of 1 mV/sec.

5.3.7 Microscopic coating morphology

Scanning electron microscopy and Energy dispersive X-ray spectroscopy (SEM-EDS) of coated samples (epoxy-clay coated system, SA-epoxy coated systems) were analysed using Carl Zeiss evo 18 instrument.

5.4 Results and discussion

5.4.1 Gas chromatography - mass spectrometry analysis (GC-MS)

The structure of the predominant biocompatible compounds is shown in **Fig. 5.2**. GC-MS chromatogram of leaves extract is depicted in **Fig. 5.3a**. Mass spectrum of 1,1,3,3-tetramethyl -1, 3-diethoxydisiloxane is portrayed in **Fig. 5.3b**. The GC-MS analysis is used to identify the organic moieties quantitatively. Peak area of the chromatogram corresponds to the amount of organic compound responsible for that peak[35]. Compounds were identified with the aid of NIST (National Institute of Standards and Technology) library. Five phyto biocompatible compounds were recognized based on their peak area percentage. The predominant compounds with their peak area % are (a) 1,1,3,3-tetramethyl- 1,3- diethoxydisiloxane (3.993), (b) hexadecanoic acid, ethyl ester (3.791), (c) butanedioic acid, hydroxy-, diethyl ester (1.650), (d) decamethylcyclo pentasiloxane (1.618), (e) ethyltetracosanoate (1.188). The peak area of the predominant compounds lies in the range of 1- 4%. Out of these, the highest peak area was possessed by 1,1,3,3–tetramethyl - 1, 3- diethoxydisiloxane (3.993) with a probability of matching 72.3%.

5.4.2 Infrared and UV-Visible spectroscopy analysis

FT-IR spectra of SA shows the presence of bands at 3650 cm^{-1}, 1766 cm^{-1}, 1468 cm^{-1}, 1061 cm^{-1} corresponding to >OH, >C=O, >C-H, >C-O vibrations. The spectrum of montmorillonite clay indicates the existence of characteristic -OH at 3700 cm^{-1}, band at

1021 cm^{-1} and 481 cm^{-1} represents Si - O and Mg - O stretching vibrations. Modified clay spectra shows band at 3529 cm^{-1}, 1750 cm^{-1}, 1469 cm^{-1}, 1021 cm^{-1} and 482 cm^{-1} corresponding to >OH, >C=O, > C- H, Si - O and Mg – O stretching vibrations. These results confirm that clay is modified in the presence of inhibitor. Spectra is presented in **Fig. 5.4**. UV-visible absorption spectrum of *S. auriculata* leaves extract in water was scrutinized. The electronic spectra of the extract show bands at 245 nm and 475 nm characteristic of π - π^* and n- π^* and is illustrated in **Fig. 5.5.**

5.4.3 Electrochemical measurements

5.4.3.1 Open circuit potential (OCP)

Prior to the start of corrosion test analysis, it is important to monitor the progress of open circuit potential till it attains a stationary steady state[36]. The OCP value was obtained by analysing the sample in a three electrode cell assembly in a potentiostat set. Nova software 2.0 was used to examine the OCP data. The variations in potential with time is measured for epoxy-clay coating and SA-epoxy coating in alkaline and acid medium and it is depicted in **Figs. 5.6a - d**. The OCP trend as observed in **Table 5.1** indicates an ascending shift in potential of SA-epoxy coated metal towards less negative (noble) direction than epoxy - clay coated samples denoting the higher corrosion resistivity in both environments. Initial OCP value of epoxy-clay coated sample is -0.41 V and SA-epoxy coating is -0.31 V in NaCl medium and for acid it is -0.51 V and -0.41 V respectively indicating cathodic shift. In general, the increase in OCP in SA-epoxy coated samples specifies the formation of enhanced protective layer on the mild steel surface. Furthermore, steady potential of OCP determines that the protective film contributes a shielding effect on the metal surface. On comparison of the datas of NaCl and H_2SO_4 corrosive mediums it is evident that in both the mediums SA-epoxy coated metals reached the noble steady state potential easily than epoxy resin coated metal thus proving their better resistance ability.

5.4.3.2 Electrochemical impedance spectroscopy (EIS)

EIS is a powerful tool used for the evaluation of the properties of polymer coated metals and their performance on exposure to aggressive environments[37-39]. The impedance values are expressed in the form of Nyquist plots. The arc in the Nyquist plots illustrates the charge transfer resistance. The inhibitive performance was investigated for epoxy-clay

coated and SA-epoxy coated systems at different intervals of time and Nyquist plots are depicted in **Figs. 5.7a-d**. Initially the charge transfer resistance of epoxy-clay coating is 42.36 Kohm cm^2 and for SA- epoxy coated metal is 75.81 Kohm cm^2 in 0.5 M NaCl. It signifies the influence of active agents existing in the inhibitor thus providing a superior protective film and active inhibition process. Greater R_{ct} values of SA-epoxy coated samples at lesser immersion time specify the enrichment of the barrier properties of the coating thus preventing the entry of water molecules providing corrosion resistance. The fall of R_{ct} values after day 1 of immersion of epoxy-clay coated samples might be due to the penetration of the electrolyte via coating. But slightly better resistance was observed in SA-epoxy coated metal (day 1) immersion which may be due to the influence of the modified clay in the epoxy coating resulting in a slight improvement in barrier properties. It can be viewed that in (day 2) the resistance of the coating in SA-epoxy sample is slightly greater in comparison with epoxy resin which is due to good dispersability throughout the coating. After (day 5) of immersion of coated metal in the alkaline and acid medium there is a reduction in the anticorrosive properties. It may be due to the penetration of corrosive chloride and sulphate ions from the electrolyte on pores of coating, decreasing the coating resistance leading to degradation of coating. In acidic environment the coating resistance of epoxy is 2.90 Kohm cm^2 and 4.02 Kohm cm^2 for SA-epoxy systems, it means that metal is more prone to corrosion in acid medium which might be due to the formation of bubbles on the coating surface and existence of pores. Decrease in C_{dl} values of SA-epoxy systems as in **Table 5.2 and 5.3** specifies the corrosion resistance and reduction in local dielectric constant[40,41]. EIS data can be demonstrated by using equivalent circuit model as depicted in **Fig. a.**

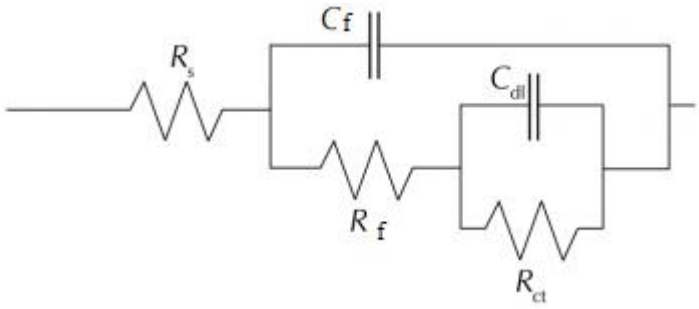

Fig. a: Equivalent circuit model

where R_s is solution resistance, C_f denotes capacitance of the coating, R_f is coating resistance, R_{ct} indicates charge transfer resistance, C_{dl} specifies double layer capacitance. A comparative result analysis of epoxy-clay coated system and the SA-epoxy coated system after immersion in alkaline and acid medium reveals that SA-epoxy coatings showed slightly higher inhibitive performance than epoxy-clay systems. This may be ascribed due to the enhanced barrier effect of the coating thereby increasing the corrosion resistance due to the combined effect of epoxy and modified nanoclay.

5.4.3.3 Bode plot

A suitable method to demonstrate impedance value is Bode method. To confirm the datas generated from the Nyquist diagrams, Bode plots were drawn for epoxy-clay coating and SA- epoxy coating in both environments. According to the previous reports, samples with higher impedance value at varying frequencies correspond to superior protective performance[42,43]. This phenomenon indicates that the coatings act as pure capacitor during the initial days of immersion. Then the impedance at the low frequencies gradually decreases with the increase of immersion time for epoxy-clay coating system. It denotes the decrease of coating protection property and the initiation of corrosion at the metal/coating interface. The impedance modulus of epoxy-clay coating indicates corrosion with increase in immersion times. By analysing the results in **Figs. 5.8a-d** it can be understood that SA-epoxy coating curves are located at higher impedance values compared to epoxy-clay system. Consequently, the barrier effect of SA- epoxy coatings was found to be slightly better which is in line with other corrosion tests. It indicates that the coating which contains corrosion inhibitor undergoes chemical reaction, and get adsorbed on the metal surface which blocks coating pores or active corrosion sites on the steel substrate.

5.4.3.4 Potentiodynamic polarisation studies

Polarisation measurements for epoxy-clay coated and SA- epoxy coated samples after immersion at different time intervals were carried out and they are portrayed in **Figs. 5.9a-d**. The polarisation datas are depicted in **Tables 5.4 and 5.5**. For comparative purpose, epoxy-clay system and SA- epoxy system Tafel datas are summarised. Evaluation of **Figs. 5.9a-d** subscribes that there is a positive shift in corrosion potential (E_{corr}) for SA-epoxy coating on mild steel (364.5 mV, 441.3 mV) than epoxy-clay coated mild steel

(481.5 mV, 509.1 mV) in alkaline and acid environment. The electrochemical parameters such as corrosion potential (E_{corr}), anodic Tafel slope (b_a) and cathodic Tafel slope (b_c) for epoxy- clay coated system and SA-epoxy coated system are obtained from the Tafel plots. The positive shift validates the formation of a protective layer[44]. In the presence of SA-epoxy samples the slightly enhanced efficiency is due to the absence of cracks, voids, contact of aggressive electrolytes to the coating surface that is arduous resulting in the improved corrosion resistance. The dispersed nanoclay along with the inhibitor in epoxy resin fills the holes and cracks thus acting as a physical barrier retarding the intrusion of corrosive ions on the metal. At lesser immersion times, diffusion of chloride, hydroxyl and sulphate ions via coating is reduced in SA-epoxy coated metal samples. It is worth noticing the shift of corrosion potential in less negative direction for SA-epoxy coated metal in comparison with epoxy-clay.

5.4.4 Microscopic coating morphology

Figs. 5.10a-b demonstrate the images analysed by SEM of epoxy coating and SA-epoxy samples on mild steel surface. It can be visualised from the images that the epoxy coating image is different from the images of SA-epoxy coated metals. It means that, SA-epoxy coated metal images with modified clay provides an enhanced protection for the metal. This enriched protection retards the entry of corrosive active species. Elemental composition of epoxy and SA-epoxy was presented in **Table 5.6.**

5.5 Mechanism of corrosion inhibition

Proposed corrosion inhibition mechanism of SA- epoxy coating on mild steel can be explained based on the above results. Dissolution of metal ions (Fe^{2+}) is reduced to some extent in SA-epoxy systems than in epoxy-clay systems. Oxygen reaching the SA-epoxy coated metal surface is less

$$Fe \longrightarrow Fe^{2+} + 2e^-$$

$$O_2 + 2H_2O + 4e^- \longrightarrow 4OH^-$$

Reduction of oxygen to hydroxides as mentioned in the above equation plays a major role in the passivation phenomenon of mild steel by generating local current that polarises the mild steel specimen into passive region. The active agents block the intrusion of anions

such as Cl^-, SO_4^{2-} and reduce the anionic concentration at the metal solution interface. It is evident from GC-MS analysis that siloxane molecules are predominant in *S. auriculata* leaves. It is well known that the insertion of active components on clay and dispersing it into the epoxy resin lead to the enhancement of the properties such as mechanical, thermal, adhesion properties as it gets adsorbed on the metal surface at one end due to the presence of hetero atoms and π-electrons held by the clay on the other end which is dispersed in the polymer matrix. This leads to a powerful adhesion between two phases of modified clay and epoxy resin takes place. A three dimensional crosslinking network takes place with epoxy, clay and inhibitor resulting in a barrier formation and prevents corrosion. Thus SA-epoxy coating provides a slightly enhanced protection than epoxy coated system. A pictorial representation for the proposed mechanism is shown in **Fig. 5.11**.

5.6 Conclusions

- GC-MS analysis revealed the presence of active components in the extract.
- IR spectra exposed the existence of functional groups.
- Results obtained based on electrochemical impedance and polarisation studies showed the slightly enhanced anti-corrosive property of SA-epoxy.
- SA-epoxy coated system is stable to some extent in alkaline than acid medium.
- SEM analysis indicates the formation of enriched protective layer due to SA-epoxy coated metal systems.
- To conclude, green inhibitor incorporated into the nanoclay and dispersed in epoxy resin provides a slightly improved corrosion resistance.

5.7 References

1. F.D. Meng, L. Liu, L.W.L. Tian, H. Wu, Y. Li, T. Zhang, F.H. Wang, Corros. Sci., **101** (2015) 139.
2. M. Kra, Z. Mandic, L. Duic, Corros. Sci., **45** (2003) 181.
3. V. Raj, R.M. Raj, Mater. Sci. Eng B., **214** (2016) 87.
4. C.K. Schoff, Prog. Org. Coat., **52** (2005) 21.
5. Y. Hao, F. Liu, E.H. Han, Prog. Org. Coat., **76** (2013) 571.
6. B. Wetzel, F. Haupert, M.Q. Zhang, Compos. Sci. Technol., **63** (2003) 2055.
7. T. Mishra, A.K. Mohanty, S.K. Tiwari, Key Engineering Materials., **571** (2013) 93.
8. M. Rahespar, F. Mohebbi, H. Hayatdavoudi, J. Alloys compd., **709** (2017) 519.
9. Y. Zhang, Y. Shao, X. Liu, C. Shi, Y. Wang, G. Meng, X. Zeng, Y. Yang, Prog. Org. Coat., **111** (2017) 240.
10. S.V. Larnaka, M.L. Zheludkevich, K.A. Yasaku, M.F. Montemor, P. Cecilio, M.G. Ferreria, Electrochem. Commun., **8** (2006) 421.
11. D. Piazza, A.F. Baldissera, S.R. Kunst, E.S. Rieder, L.C. Scienza, C.A. Ferreira, A.J. Zattera, Mater. Res., **18** (2015) 897.
12. A. Toloei, S. Atashin, M.E. Bahrololoom, Mat. Sci., **2013** (2013) 1.
13. T.A. Truc, T.T.X. Hang, V.K. Oanh, Surf. Coat. Tech., **202** (2008) 4945.
14. S.E. Vidotti, A.C. Chinellato, G. Hu, L.A. Pessanc, Mater. Res., **20** (2017) 826.
15. M. Monisha, M. Sowmiya, R. Ragunathan, J. Johney, Int. J. Curr. Microbiol. App. Sci., **6** (2017) 425.
16. A. Raju, V. Lakshmi, R.K.V. Prataap, V.G. Resmi, T.P.D. Rajan, C. Pavithran, V.S. Prasad, S. Mohan, Appl Clay Sci., **126** (2016) 81.
17. M.G. Hosseini, K. Aboutalebi, Prog. Color Colorants Coat., **10** (2017) 181.
18. M.S. Vijaykumar, R. Saravanan, IJMET., **8** (2017) 1105.

19. W.B. WanNik, H.M. Hajar, M.J. Suriani, M.G.M. Sabri, M.J. Ghazali, JMES., **11** (2017) 3179.

20. S. Ghodrati, A. Mahmoodi, M. Mohseni, Clay Minerals., **53** (2018) 60.

21. N. Relosi, O.A. Neuwald, A.J. Zattera, D. Piazza, S.R. Kunst, E.J. Birriel, Polimeros., **28** (2018) 355.

22. M.K. Madhup, N.K. Shah, N.R. Parekh, Mat. Sci. Res. India., **15** (2018) 165.

23. R. Shankar, K.G. Manjunath, A.K. Shuka, K.S. Badari Narayan, IJESRT., **7** (2018) 355.

24. K. Jlassi, A.B. Radwan, K.K. Sadasivuni, M. Mrlik, A.M. Abdullah, M.M. Chehimi, Krupa, Sci. Rep., **8** (2018) 1 DOI:10.1038/s41598-018-31508-0.

25. S. Gul, A. Kausar, B. Muhammad, S. Jabeen, M. Farooq, M. Kashif, AJPSE., **6** (2018) 1.

26. Mahmoodi, E. Ebrahimi, A. Khosravi, Prog. Org. Coat., **119** (2018) 164.

27. M. Rudresh, B.H. Maruthi, H.P. Nagaswarupa, B.S. Surendra, M.R. AnilKumar, N. Raghavendra, AJEAT., **8** (2019) 32.

28. T.A. Nguyen, Q.T. Nguyen, T.P. Bach, Int. J. Chem., **2019** (2019) 1.

29. E. Akbarinezhad, Corros Eng Sci Techn (2019) DOI:10.1080/147822X. 2019.1599177.

30. J. Zhang, H. Huang, J. Ma, L. Huang, L. Huang, X. Chen, H. Zeng, S. Ma, Front Mater., **6** (2019) 1.

31. S.M. Kabeb, A. Hassan, Z. Mohamad, Z. Sharer, M. Mokhtar, F. Ahmad, Chem. Eng. Trans., **72** (2019) 121.

32. T.A. Truc, T.T. Thuy, V.K. Oanh, T.T.X. Hang, A.S. Nguyen, N. Causse, N. Pebere, Surf. Interface. Anal., **14** (2019) 26.

33. T.T.X. Hang, T.A. Truc, M.G. Olivier, C. Vandemiers, Prog. Org. Coat., **69** (2010) 410.

34. S.P. Ali, C.D. Dehghanian, A. Kosari, Corros. Sci., **85** (2014) 204.

35. S. Leelavathi, R. Rajalakshmi, J. Mater. Environ. Sci., **4** (2013) 625.

36. L. Mardare, L. Benea, IOP. Confser. Mater. Sci. Eng., **209** (2017) 1.

37. K. Indira, T. Nishimura, Int. J. Electrochem. Sci., **11** (2016) 419.

38. R. Hsissou, B. Benzidia, N. Hajjaji, A. Elharfi, JCTM., **53** (2018) 898.

39. T. Balusamy, T. Nishimura, Am. J. Analyt. Chem., **7** (2016) 533.

40. Z. Mahidashti, T. Shahrabi, B. Ramezanzadeh, Appl. Surf. Sci., **390** (2016) 623.

41. M. Outirite, Lagrenee, M. Lebrini, M. Traisnel, C. Jama, H. Vezin, F. Bentiss, Electrochim. Acta., **55** (2010) 1670.

42. J.M. Yeh, H.Y. Huang, C.I. Chen, W.F. Su, Y.H Yu, Surf. Coat. Tech., **200** (2006) 2753.

43. S. Bera, T.K. Rout, G. Udayabhanu, R. Narayan, Prog. Org. Coat., **101** (2016) 24.

44. S.E. Vidotti, A.C. Chinellato, G. Hu, L.A. Pessanc, Mater. Res., **20** (2017) 826.

Table 5.1: Open circuit potential values

Time (days)	OCP(V) epoxy-clay (NaCl)	OCP(V) SA-epoxy (NaCl)	OCP(V) epoxy-clay (Acid)	OCP(V) SA-epoxy (Acid)
Day 1	-0.41	-0.31	-0.51	-0.41
Day 2	-0.42	-0.35	-0.53	-0.51
Day 3	-0.50	-0.42	-0.55	-0.52
Day 4	-0.51	-0.50	-0.56	-0.54
Day 5	-0.61	-0.57	-0.63	-0.60

Table 5.2: AC-impedance parameters of coated samples (epoxy-clay and SA-epoxy) at different immersion times in NaCl medium

Immersion time (days)	Sample	R_{ct} (Kohm cm^2)	C_{dl} (µF/cm^2)
Day 1	epoxy-clay	42.36	9.24
	SA-epoxy	75.81	3.68
Day 2	epoxy-clay	34.54	14.67
	SA-epoxy	62.95	7.92
Day 3	epoxy-clay	17.51	28.73
	SA-epoxy	44.52	12.64
Day 4	epoxy-clay	9.11	47.87
	SA-epoxy	21.06	17.52
Day 5	epoxy-clay	7.55	52.67
	SA-epoxy	11.37	34.26

Table 5.3: AC-impedance parameters of coated samples (epoxy-clay and SA-epoxy) at different immersion times in acid medium

Immersion time (days)	Sample	R_{ct} (Kohm cm^2)	C_{dl} (µF/cm^2)
Day 1	epoxy-clay	2.90	70.58
	SA-epoxy	4.02	53.27
Day 2	epoxy-clay	1.74	81.10
	SA-epoxy	3.16	58.29
Day 3	epoxy-clay	1.26	89.97
	SA-epoxy	1.44	82.24
Day 4	epoxy-clay	0.65	94.72
	SA-epoxy	0.86	90.28
Day 5	epoxy-clay	0.31	98.53
	SA-epoxy	0.37	92.62

Table 5.4: Corrosion parameters for coated samples (epoxy-clay and SA-epoxy) at different immersion times in NaCl medium

Immersion time (days)	Sample	Tafel slopes(mV/dec)		$-E_{corr}$ (mV)
		b_a	b_c	
Day 1	epoxy-clay	65	140	481.5
	SA-epoxy	67	120	364.5
Day 2	epoxy-clay	54	135	518.1
	SA-epoxy	51	125	398.1
Day 3	epoxy-clay	47	160	522.9
	SA-epoxy	40	142	422.4
Day 4	epoxy-clay	44	175	604.9
	SA-epoxy	49	151	543.9
Day 5	epoxy-clay	45	185	630.6
	SA-epoxy	38	164	603.8

Table 5.5: Corrosion parameters for coated samples (epoxy-clay and SA-epoxy) at different immersion times in acid medium

Immersion time (days)	Sample	Tafel slopes (mV/dec)		$-E_{corr}$ (mV)
		b_a	b_c	
Day 1	epoxy-clay	51	173	509.1
	SA-epoxy	45	176	441.3
Day 2	epoxy-clay	55	168	506.7
	SA-epoxy	51	170	483.6
Day 3	epoxy-clay	62	157	511.4
	SA-epoxy	64	161	497.7
Day 4	epoxy-clay	71	145	525.6
	SA-epoxy	74	151	496.4
Day 5	epoxy-clay	86	138	640.3
	SA-epoxy	91	146	567.0

Table 5.6: Elemental composition

Element (Wt %)	epoxy	SA-epoxy
C	68.14	76.23
O	31.86	20.94
Si	-	2.83

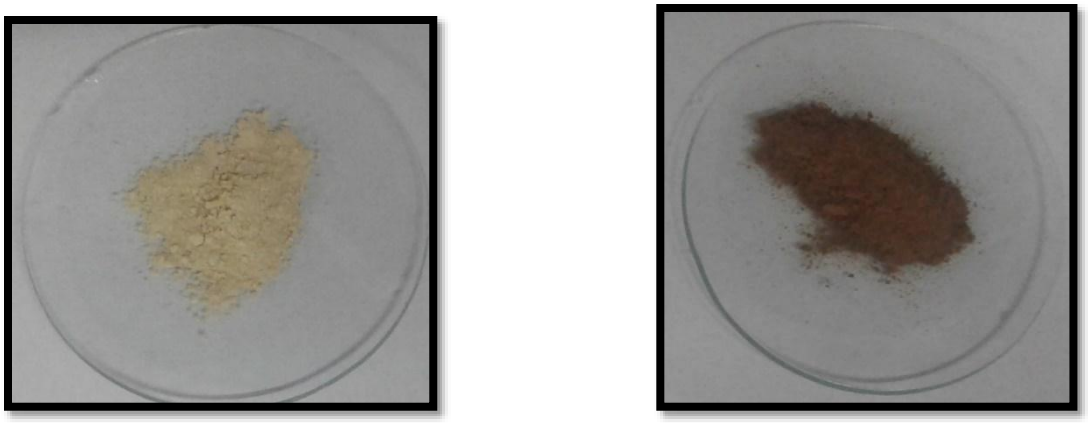

(a) **(b)**

Fig. 5.1: Images of (a) nano clay and (b) SA-modified nanoclay

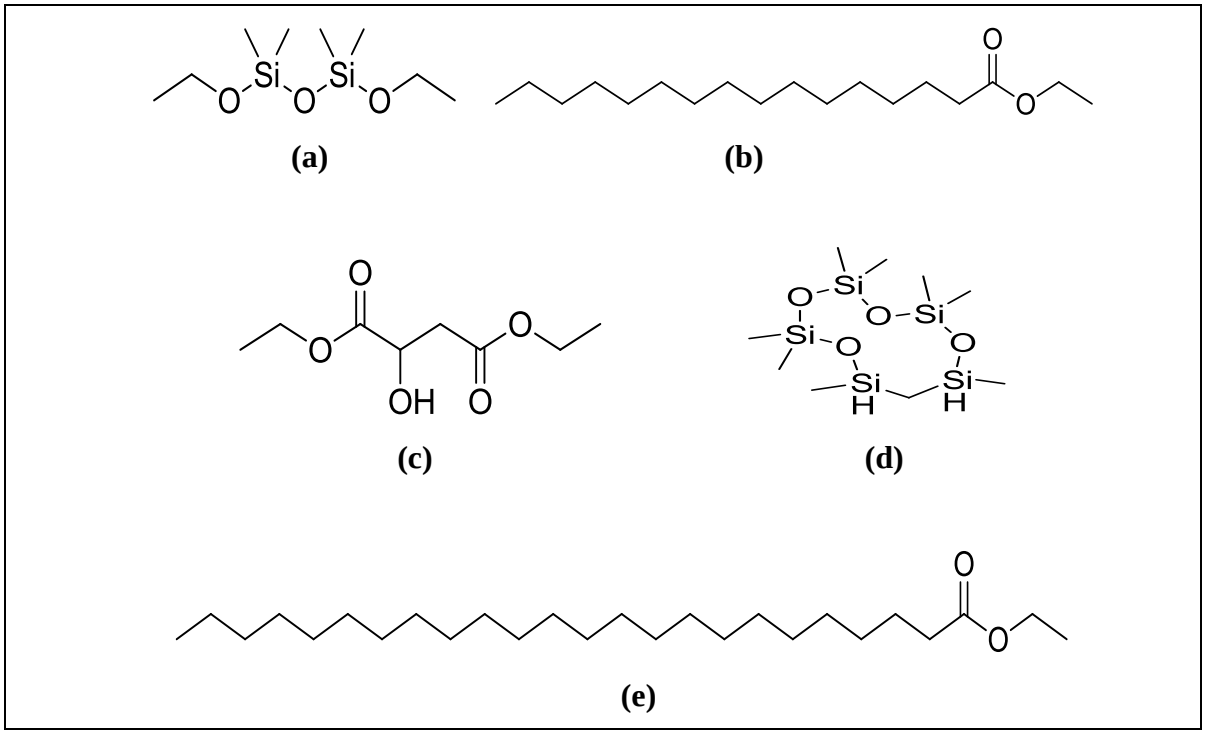

Fig. 5.2: Structure of predominant compounds in *Senna auriculata*

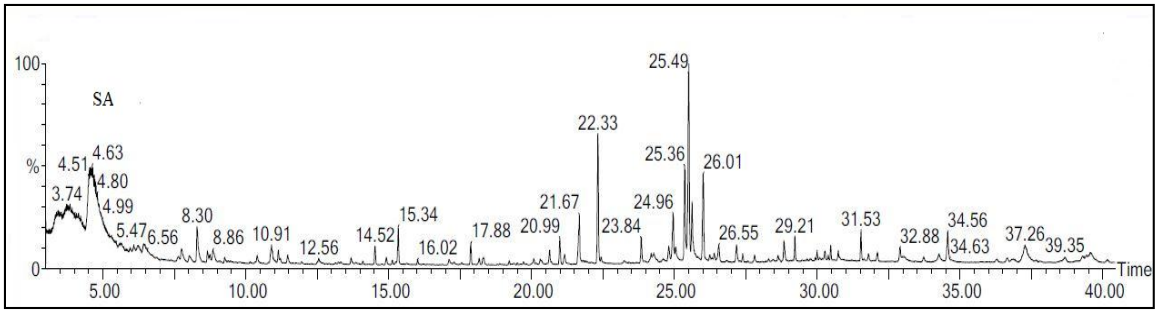

Fig. 5.3(a): GC-MS Chromatogram of *Senna auriculata*

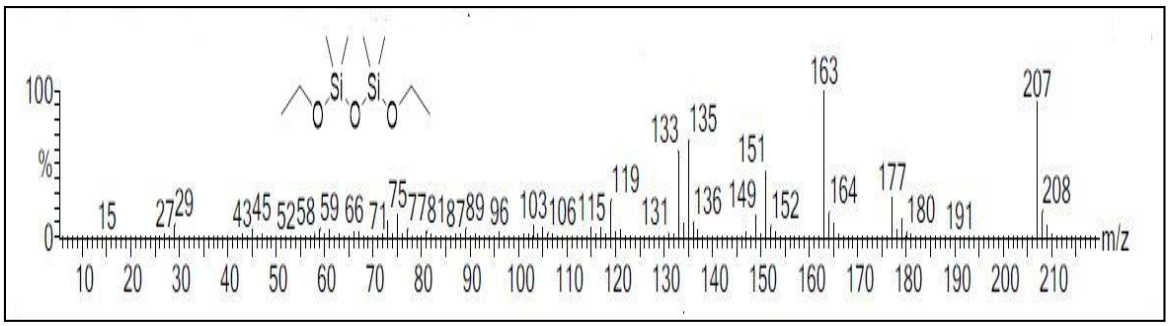

Fig. 5.3(b): Mass spectrum of 1,1,3,3- tetramethyl -1,3-diethoxydisiloxane

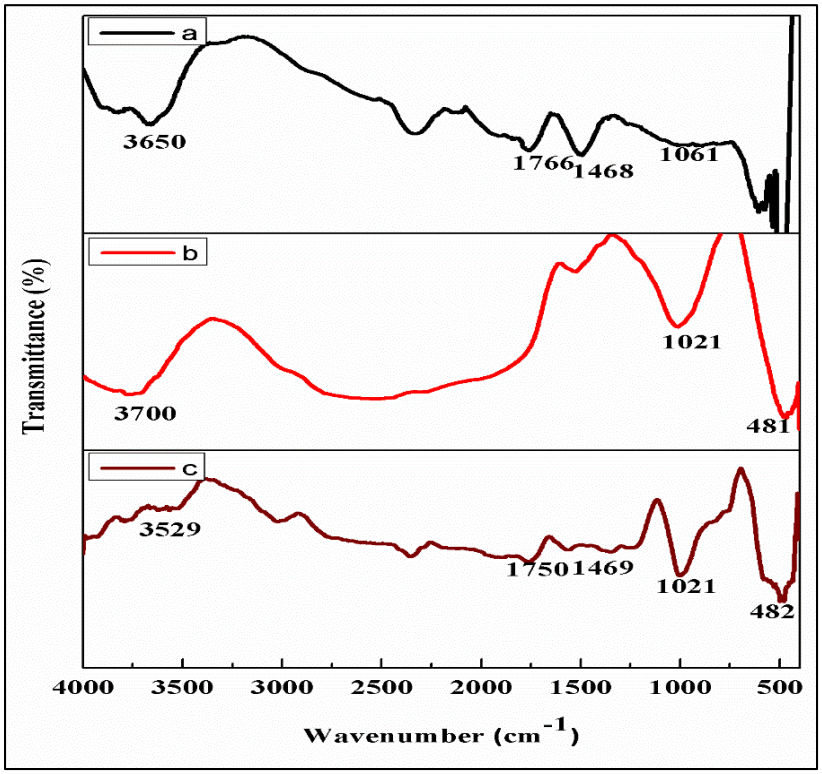

Fig. 5.4: IR spectra of (a) SA (b) montmorillonite nanoclay (c) modified nanoclay

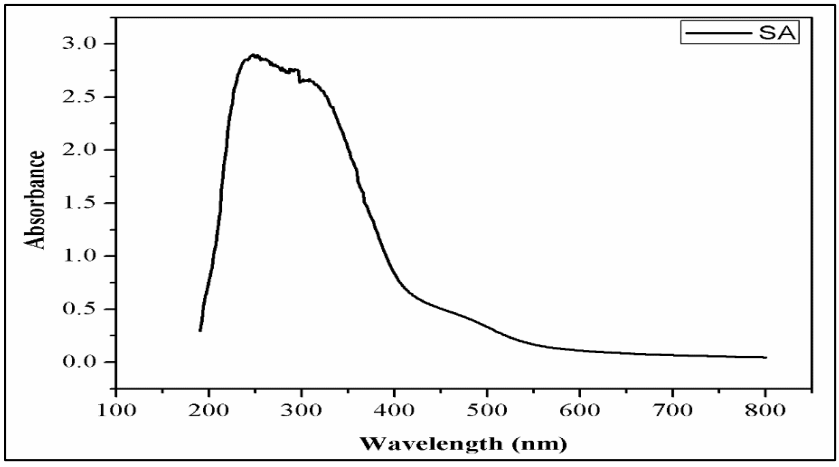

Fig. 5.5: UV-visible spectrum of *S. auriculata* leaf extract

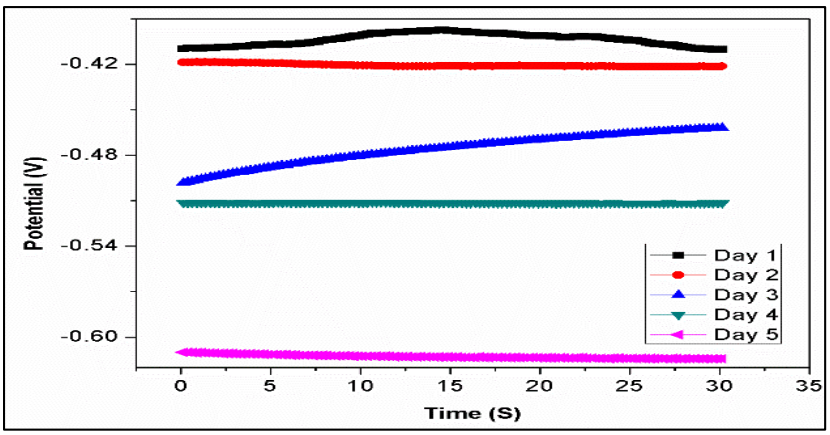

Fig. 5.6(a): Variation of open circuit potential with time of epoxy–clay coated metal system immersed in 0.5 M NaCl solution

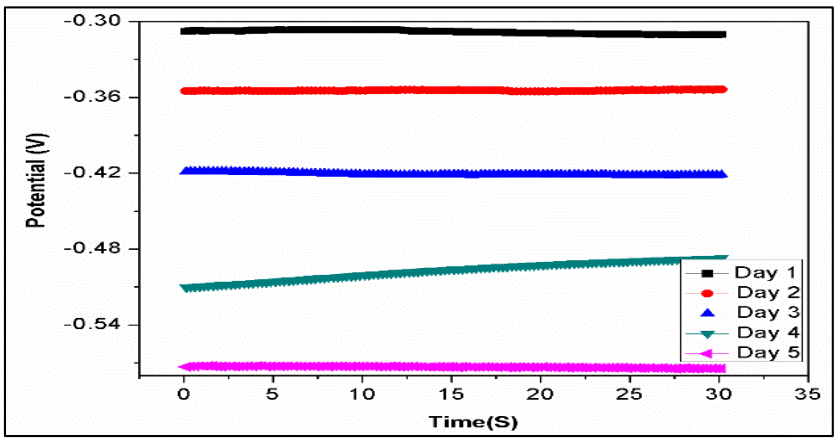

Fig. 5.6(b): Variation of open circuit potential with time of SA-epoxy coated metal system immersed in 0.5 M NaCl solution

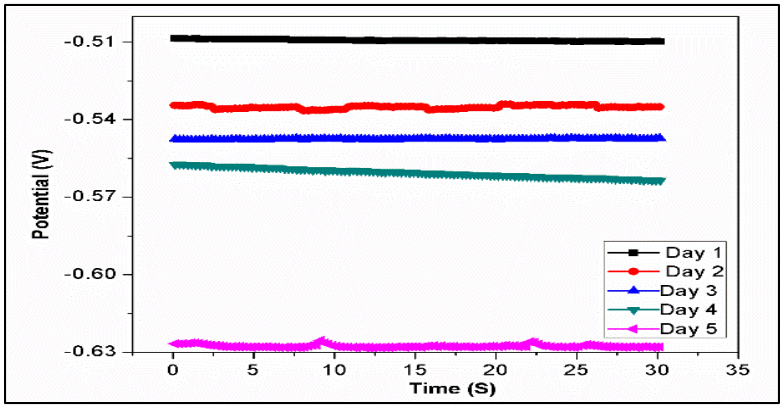

Fig. 5.6(c): Variation of open circuit potential with time of epoxy-clay coated metal systems immersed in 0.5 M H_2SO_4 solution

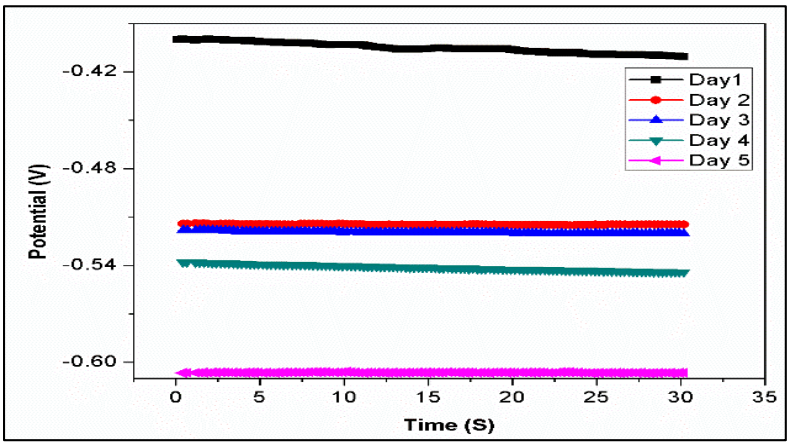

Fig. 5.6(d): Variation of open circuit potential with time of SA-epoxy coated metal systems immersed in 0.5 M H_2SO_4 solution

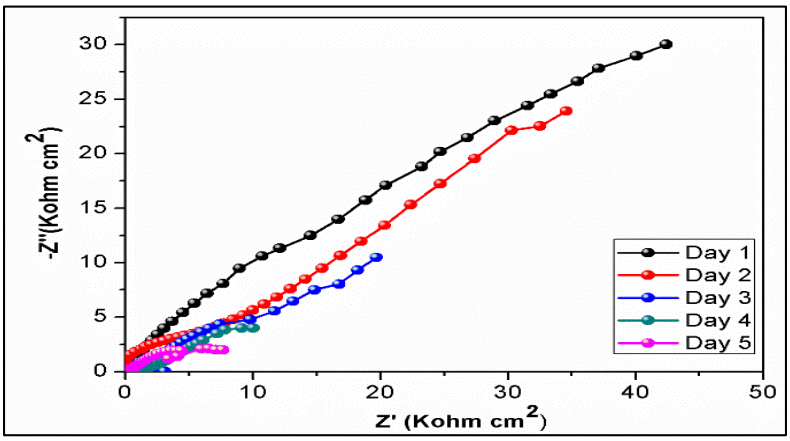

Fig. 5.7(a): Nyquist impedance spectra of epoxy-clay coated/metal systems in 0.5 M NaCl

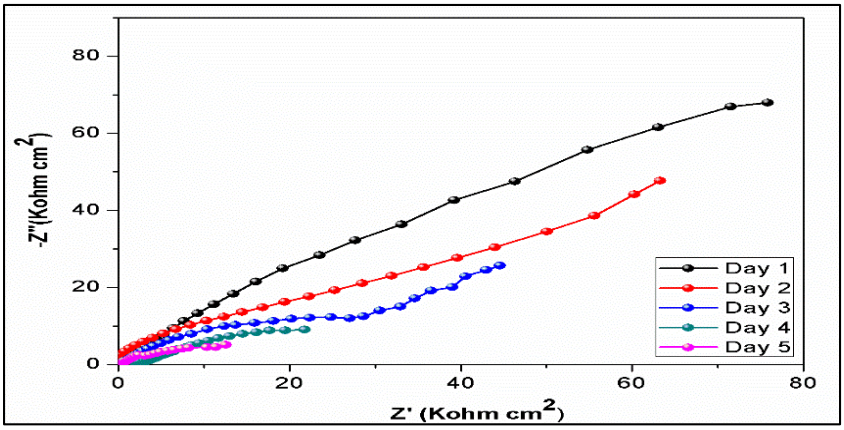

Fig. 5.7(b): Nyquist impedance spectra of SA- epoxy coated/metal systems in 0.5 M NaCl

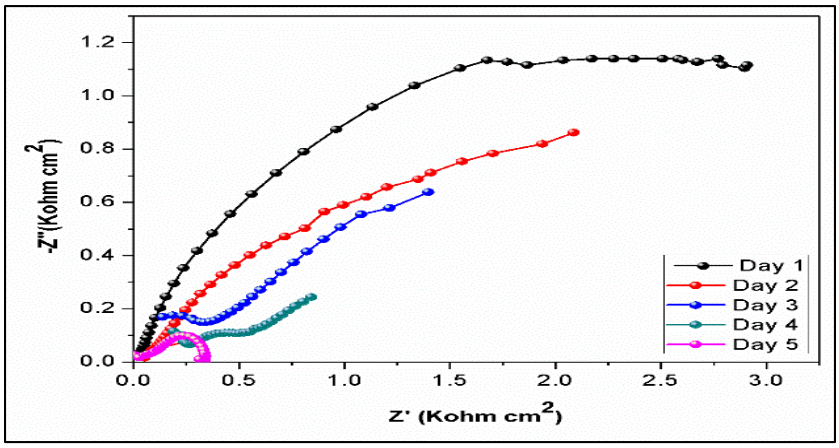

Fig. 5.7(c): Nyquist impedance spectra of epoxy-clay coated/metal systems in 0.5 M H_2SO_4

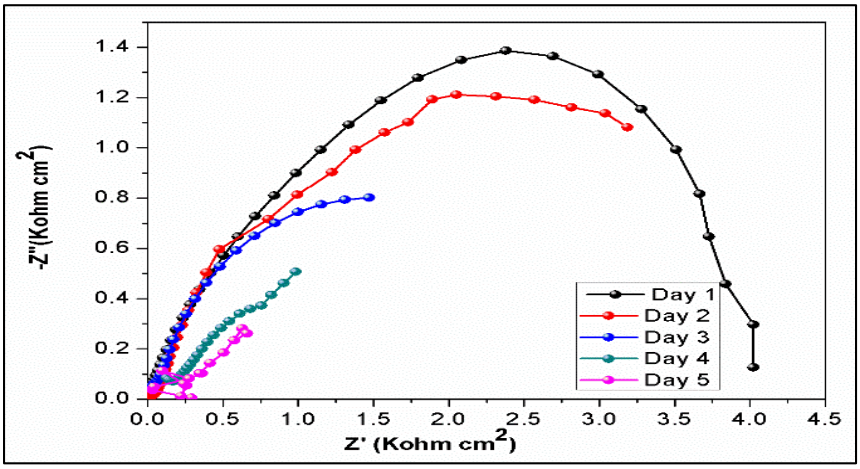

Fig. 5.7(d): Nyquist impedance spectra of SA-epoxy coated/metal systems in 0.5 M sulphuric acid

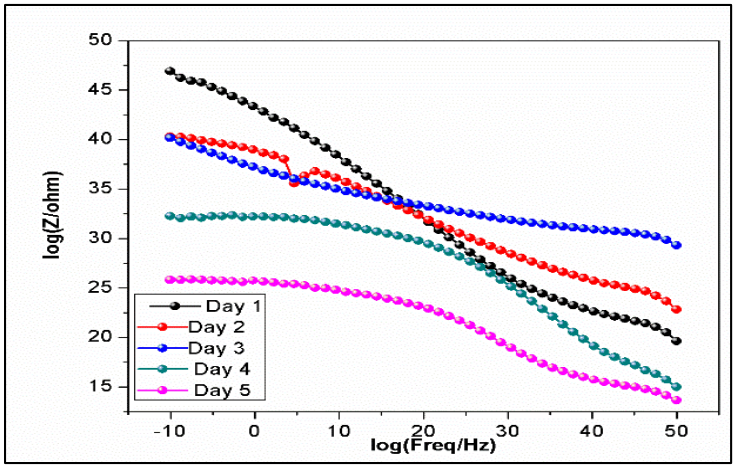

Fig. 5.8(a): Bode impedance plots of epoxy-clay coated metal systems in 0.5 M NaCl

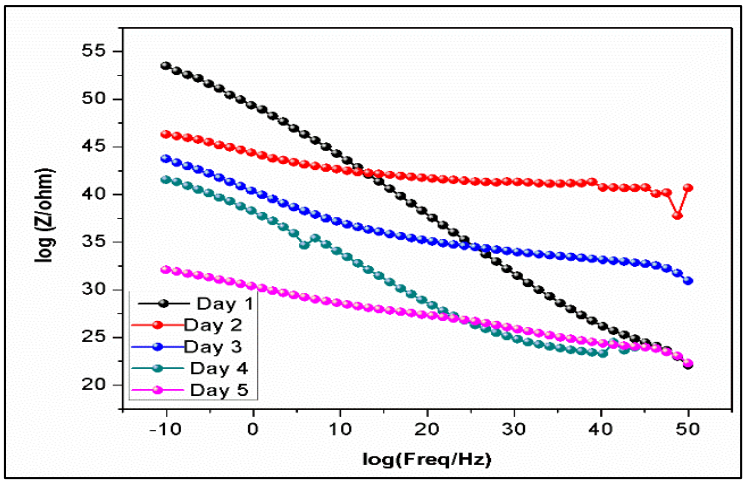

Fig. 5.8(b): Bode impedance plots of SA-epoxy coated metal systems in 0.5 M NaCl

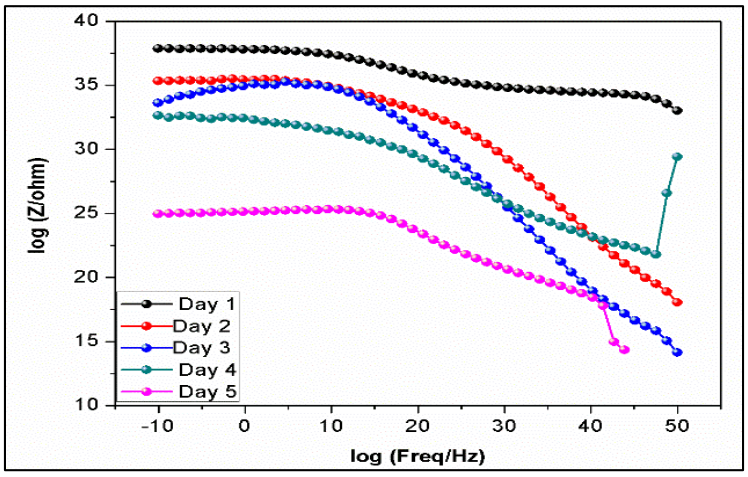

Fig. 5.8(c): Bode impedance plots of epoxy-clay coated/metal systems in 0.5 M H_2SO_4

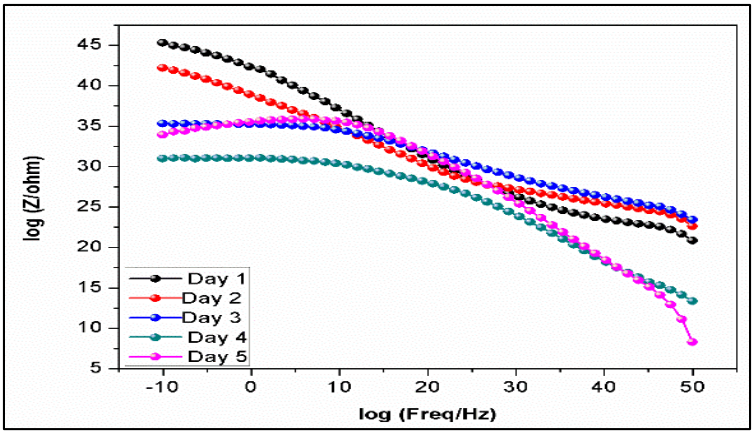

Fig. 5.8(d): Bode impedance plots of SA-epoxy coated/metal systems in 0.5 M H_2SO_4

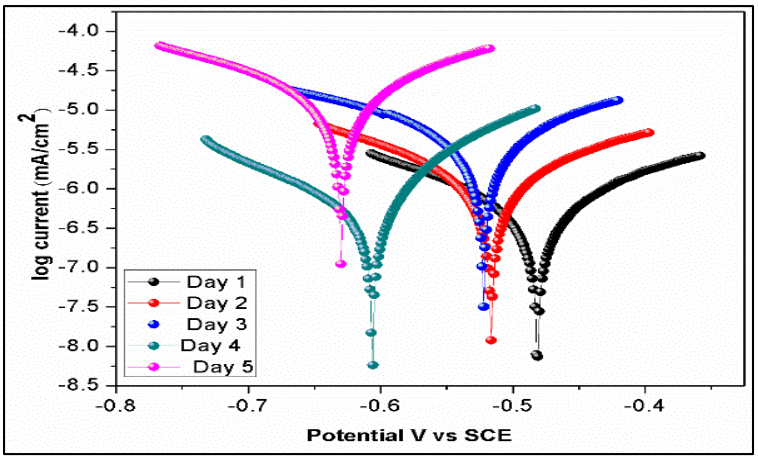

Fig. 5.9(a): Potentiodynamic polarisation curves of epoxy-clay coated metal systems in 0.5 M NaCl

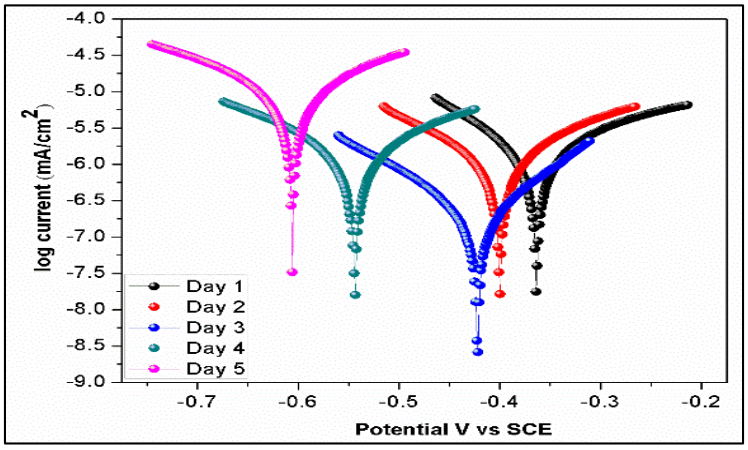

Fig. 5.9(b): Potentiodynamic polarisation curves of SA-epoxy coated metal systems in 0.5 M NaCl

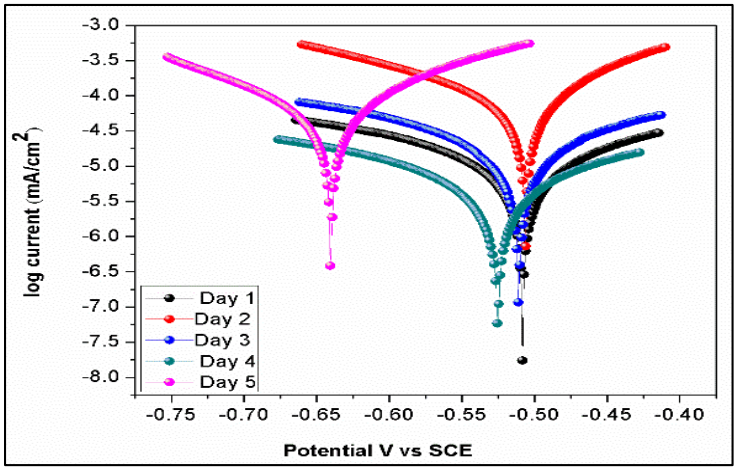

Fig. 5.9(c): Potentiodynamic polarisation curves of epoxy-clay coated metal systems in 0.5 M H_2SO_4

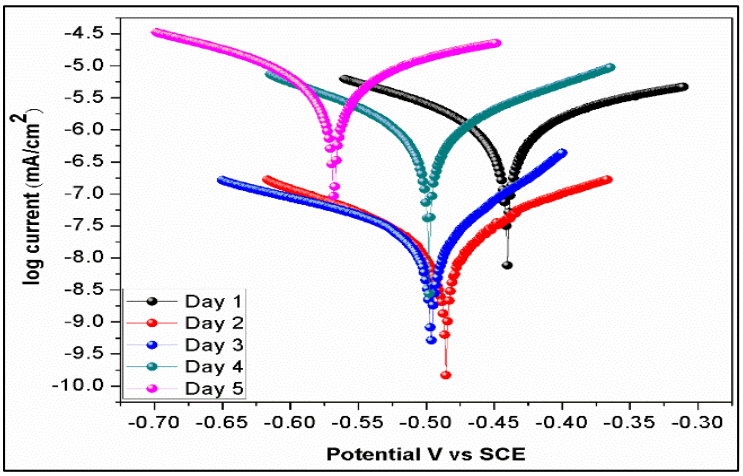

Fig. 5.9(d): Potentiodynamic polarisation curves of SA- epoxy coated metal systems in 0.5 M H_2SO_4

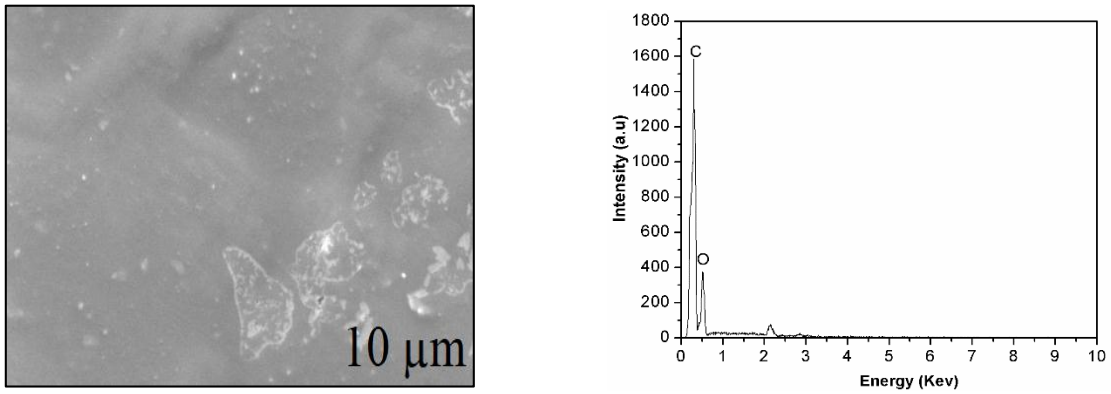

(a)

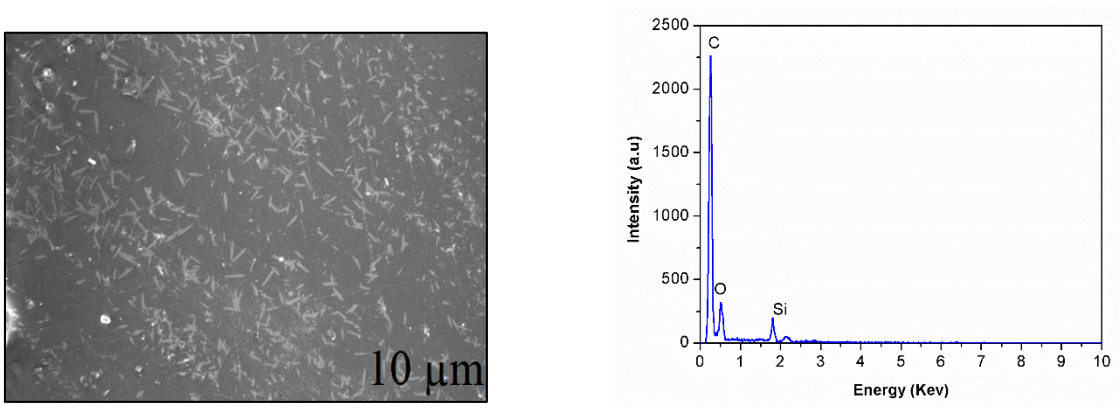

(b)

Fig. 5.10: SEM – EDS spectra of (a) epoxy coated samples (b) SA-epoxy coated samples

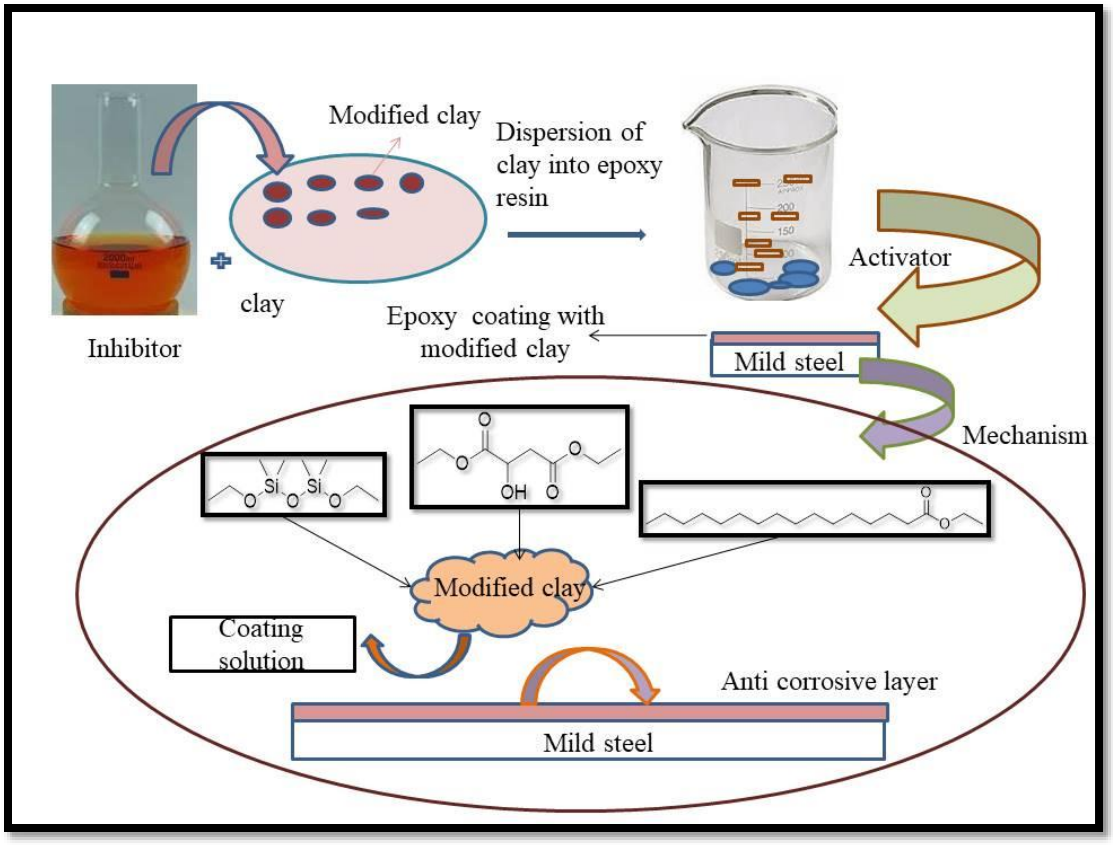

Fig. 5.11: Schematic representation of proposed mechanism of inhibition